Am J Physiol Renal Physiol 310: F895–F908, 2016.
First published February 17, 2016; doi:10.1152/ajprenal.00431.2015.

Loss of diacylglycerol kinase epsilon in mice causes endothelial distress and impairs glomerular Cox-2 and PGE_2 production

Jili Zhu,[1,2]* Moumita Chaki,[1,3]* Dongmei Lu,[1] Chongyu Ren,[1] Shan-Shan Wang,[1] Alysha Rauhauser,[1] Binghua Li,[1] Susan Zimmerman,[1] Bokkyoo Jun,[4] Yong Du,[5] Komal Vadnagara,[1] Hanquin Wang,[1,6] Sarah Elhadi,[1,7] Richard J. Quigg,[8] Matthew K. Topham,[9] Chandra Mohan,[5] Fatih Ozaltin,[10,11] Xin J. Zhou,[12] Denise K. Marciano,[1] Nicolas G. Bazan,[4] and Massimo Attanasio[1,13]

[1]*Department of Internal Medicine, University of Texas Southwestern Medical Center, Dallas, Texas;* [2]*Department of Nephrology, Renmin Hospital, Wuhan University, Hubei, Wuhan, China;* [3]*Department of Neuroscience, University of Texas Southwestern Medical Center, Dallas, Texas;* [4]*Department of Neuroscience, Louisiana State University, New Orleans, Louisiana;* [5]*Biomedical Engineering, University of Houston, Houston, Texas;* [6]*Institute of Basic Medical Sciences, Hubei University of Medicine, Hubei, Shiyan, China;* [7]*Department of Pediatrics, University of Texas Southwestern Medical Center, Dallas, Texas;* [8]*Department of Medicine, University of Buffalo, Buffalo, New York;* [9]*Huntsman Cancer Institute, University of Utah, Salt Lake City, Utah;* [10]*Department of Pediatric Nephrology, Faculty of Medicine, Hacettepe University, Ankara, Turkey;* [11]*Nephrogenetics Laboratory, Department of Pediatric Nephrology, Faculty of Medicine, Hacettepe University, Ankara, Turkey;* [12]*Renal Path Diagnostics, Pathologist BioMedical Laboratories and Department of Pathology, Baylor University Medical Center, Dallas, Texas; and* [13]*Eugene McDermott Center for Growth and Development, The University of Texas Southwestern Medical Center, Dallas, Texas*

Submitted 23 September 2015; accepted in final form 23 January 2016

Zhu J, Chaki M, Lu D, Ren C, Wang S, Rauhauser A, Li B, Zimmerman S, Jun B, Du Y, Vadnagara K, Wang H, Elhadi S, Quigg RJ, Topham MK, Mohan C, Ozaltin F, Zhou XJ, Marciano DK, Bazan NG, Attanasio M. Loss of diacylglycerol kinase epsilon in mice causes endothelial distress and impairs glomerular Cox-2 and PGE_2 production. *Am J Physiol Renal Physiol* 310: F895–F908, 2016. First published February 17, 2016; doi:10.1152/ajprenal.00431.2015.—Thrombotic microangiopathy (TMA) is a disorder characterized by microvascular occlusion that can lead to thrombocytopenia, hemolytic anemia, and glomerular damage. Complement activation is the central event in most cases of TMA. Primary forms of TMA are caused by mutations in genes encoding components of the complement or regulators of the complement cascade. Recently, we and others have described a genetic form of TMA caused by mutations in the gene diacylglycerol kinase-ε (*DGKE*) that encodes the lipid kinase DGK_ε (Lemaire M, Fremeaux-Bacchi V, Schaefer F, Choi MR, Tang WH, Le Quintrec M, Fakhouri F, Taque S, Nobili F, Martinez F, Ji WZ, Overton JD, Mane SM, Nurnberg G, Altmuller J, Thiele H, Morin D, Deschenes G, Baudouin V, Llanas B, Collard L, Majid MA, Simkova E, Nurnberg P, Rioux-Leclerc N, Moeckel GW, Gubler MC, Hwa J, Loirat C, Lifton RP. *Nat Genet* 45: 531–536, 2013; Ozaltin F, Li BH, Rauhauser A, An SW, Soylemezoglu O, Gonul II, Taskiran EZ, Ibsirlioglu T, Korkmaz E, Bilginer Y, Duzova A, Ozen S, Topaloglu R, Besbas N, Ashraf S, Du Y, Liang CY, Chen P, Lu DM, Vadnagara K, Arbuckle S, Lewis D, Wakeland B, Quigg RJ, Ransom RF, Wakeland EK, Topham MK, Bazan NG, Mohan C, Hildebrandt F, Bakkaloglu A, Huang CL, Attanasio M. *J Am Soc Nephrol* 24: 377–384, 2013). DGK_ε is unrelated to the complement pathway, which suggests that unidentified pathogenic mechanisms independent of complement dysregulation may result in TMA. Studying *Dgke* knockout mice may help to understand the pathogenesis of this disease, but no glomerular phenotype has been described in these animals so far. Here we report that *Dgke* null mice present subclinical microscopic anomalies of the glomerular endothelium and basal membrane that worsen with age and develop glomerular capillary occlusion when exposed to nephrotoxic serum. We found that induction of cyclooxygenase-2 and of the proangiogenic prostaglandin E_2 are impaired in *Dgke* null kidneys and are associated with reduced expression of the antithrombotic cell adhesion molecule platelet endothelial cell adhesion molecule-1/CD31 in the glomerular endothelium. Notably, prostaglandin E_2 supplementation was able to rescue motility defects of *Dgke* knockdown cells in vitro and to restore angiogenesis in a test in vivo. Our results unveil an unexpected role of *Dgke* in the induction of cyclooxygenase-2 and in the regulation of glomerular prostanoids synthesis under stress.

thrombotic microangiopathy; *DGKE*; hemolytic uremic syndrome

THROMBOTIC MICROANGIOPATHY (TMA) is a disorder associated with high mortality and substantial risk of progressing to chronic kidney disease (29). TMA is characterized by damage of the small vasculature of multiple organs, platelet aggregation, and arteriolar and capillary thrombosis, with consequent thrombocytopenia, microangiopathic hemolytic anemia, and organ damage (11). TMA is a common manifestation to several primary diseases, including hemolytic uremic syndrome (HUS), secondary or not to Shiga toxin-producing *E. coli* infections, thrombotic thrombocytopenic purpura, malignant hypertension, and preeclampsia. With the exception of thrombotic thrombocytopenic purpura, in which severe acute kidney injury and progression to chronic kidney disease are rare (15), kidney function is invariably affected in all of these conditions, suggesting that glomerular capillaries are particularly susceptible to develop thrombotic lesions (9, 17). Activation of the complement cascade is the central event of several forms of TMA (35). Infections from Shiga-like toxin-producing bacteria (Shiga-toxin *E. coli*-HUS), for example, result in excessive complement activation with consequent endothelial cell damage and exposure of tissue factor, thrombin, and other molecules that contribute to the formation of microthrombi (26). HUSs not associated with bacterial infection are defined atypical (atypical HUS) and are most often secondary to defects in

* J. Zhu and M. Chaki contributed equally to this work.

Address for reprint requests and other correspondence: M. Attanasio, Internal Medicine, Eugene McDermott Center for Growth and Development, Univ. of Texas Southwestern Medical Center, 5323 Harry Hines Blvd., Dallas, TX, 75390 (e-mail: massimo.attanasio@utsouthwestern.edu).

genes encoding factors that participate in the complement cascade (30). Recently, our laboratory and others have described a genetic form of TMA that is caused by mutations in the gene that encodes the lipid kinase diacylglycerol kinase-ε (DGK_ε), and it is unrelated to the complement pathway (20, 31, 42). Recessive loss of function mutations in the *DGKE* gene cause TMA with histological features (increased deposition of mesangial matrix, thickening of the glomerular capillary walls, and splitting of the glomerular basement membrane) that resemble membrano-proliferative glomerulonephritis, but the mechanisms that lead to this disease are still unexplained (20, 31, 42). DGKs are intracellular lipid kinases devoted to phosphorylate diacylglycerol (DAG) to phosphatidic acid (36). At least 10 DGKs have been identified in mammals, differing mostly for the composition of the noncatalytic domains, which confer specific activity to each isoform (24). The epsilon isoform is a ubiquitous enzyme with higher level of expression in testis, cardiac and skeletal muscle, and kidney, where it has been demonstrated in podocytes and endothelial cells (20, 31). DGK_ε is constitutively active and has high specificity for DAG

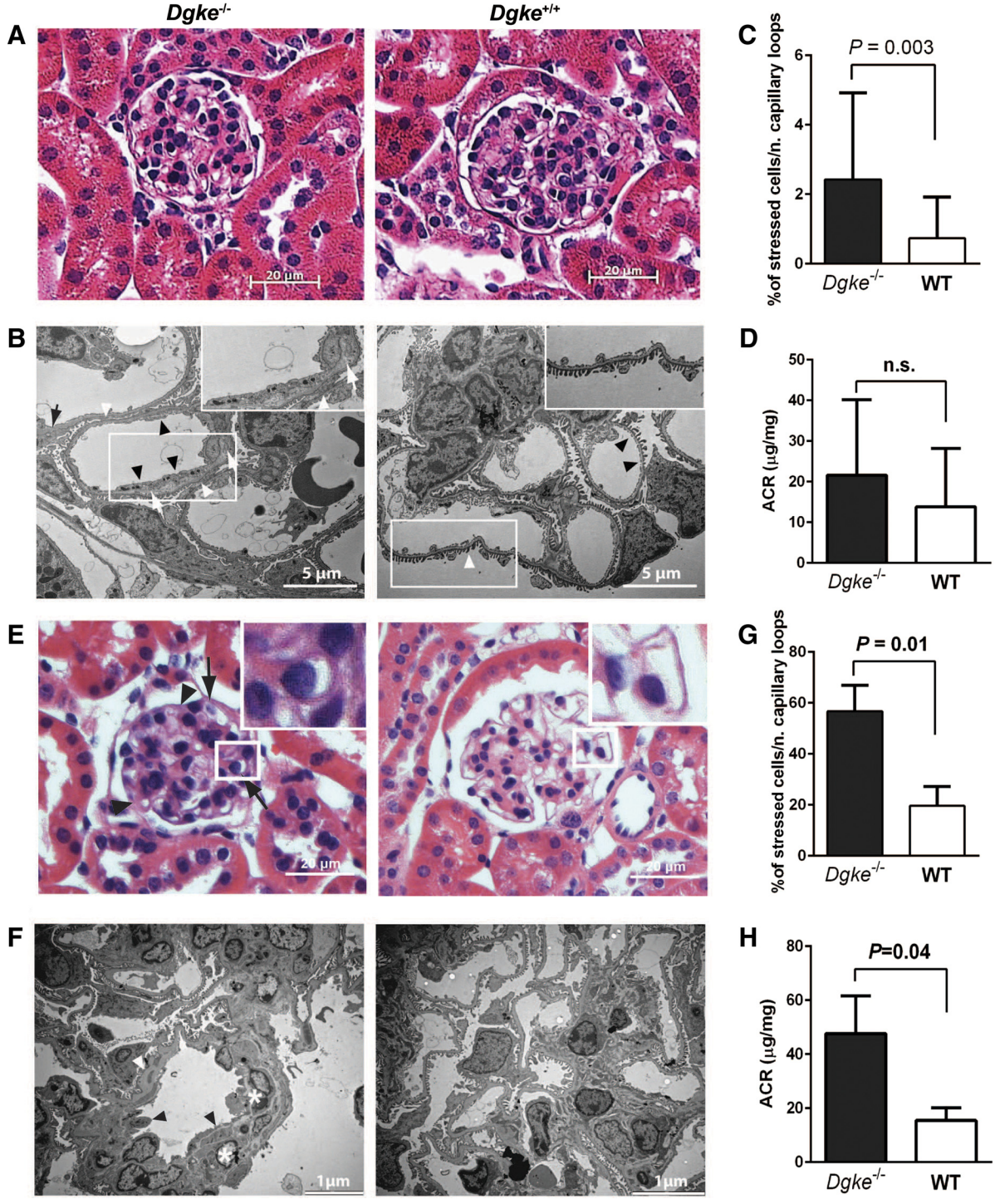

acylated with arachidonic acid (AA) in *sn*-2 position (*sn*-2-arachidonoyl-DAG). The high substrate selectivity, together with the constitutive activation of this enzyme, results in enrichment of the cellular polyphosphatidylinositides with AA acyl chains (25, 41). AA is the main precursor in the production of prostaglandins (PGs), and its cellular availability is the rate-limiting factor for the synthesis of prostanoids (19). PG synthesis is usually triggered by activation of membrane phospholipase A2 that releases AA from phospholipids in the cell membrane (19). Then the inducible enzyme PG endoperoxide synthase 2, also known as cyclooxygenase-2 (Cox-2), converts AA to the intermediate PG H_2 (PGH_2) that is, in turn, metabolized by specific PG synthases into PG E_2 (PGE_2), PG I_2 (PGI_2), thromboxane A2 (TxA_2), $PGF_{2\alpha}$, and PGD_2 (12). PGs are short-lived ubiquitous signaling molecules that are important mediators in kidney physiology and pathology and are required for microvascular angiogenesis and function (12, 34). Inactivation of *Dgke* in mice has been shown to affect recovery from seizures after brain electrogenic stimulation, but no glomerular phenotype has been described. Since mutations in humans result in TMA, we hypothesized that loss of *Dgke* in mice may cause subclinical glomerular lesions and may predispose to disease. Here we report that *Dgke* knockout mice have subclinical microscopic anomalies of the glomerular endothelium and basal membrane that worsen with age and develop extensive glomerular capillary occlusion when challenged with nephrotoxic serum (NS). We found that *Dgke* knockout mice fail to induce glomerular *Cox-2* and the pro-angiogenic prostanoid PGE_2 after puromycin aminonucleoside (PAN)-mediated glomerulonephritis. Concordantly, with the reduced expression of *Cox-2*, *Dgke* knockout mice were partially protected from developing podocyte foot process effacement and proteinuria after PAN injury. *Dgke* knockout mice also showed reduced expression of the antithrombotic cell adhesion molecule platelet endothelial cell molecule-1 (PECAM-1) in the glomerular endothelium. Notably, PGE_2 supplementation was able to rescue motility defects of *Dgke* knockdown cells in vitro and to restore angiogenesis in an in vivo test. Our results suggest that *Dgke* has both endothelial and podocyte-specific functions, and that it is required for glomerular induction of Cox-2 and synthesis of vasoactive prostanoids.

MATHERIALS AND METHODS

Mice knockouts. Dgke knockout mice were developed on a C57/B6 background and have been previously described (36). All of the experiments were previously approved by the Institutional Animal Care and Use Committee of University of Texas Southwestern Medical Center.

NS and PAN-induced glomerulonephritis. Glomerular basal membrane (GBM)-reactive NS was generated by Lampire Laboratories (Pipersville, PA), as previously described (43). Mice were challenged with intraperitoneal injections of complete Freund adjuvant, then with a first dose of NS (12.5 μg/g), followed by a second dose (5 μg/g) after 5 days. Equal amount of nonimmune isotypic serum (NIS) was used as a control. Fourteen days later, 24-h urine was collected, and kidneys were harvested for fixation or glomeruli isolation. PAN (Sigma, St. Louis, MO) was administered by intraperitoneal injection at the dose of 0.5 $mg \cdot g^{-1} \cdot day^{-1}$ for 2 days. An equal amount of volume per gram of body weight of saline was injected as a control. Mice were killed 3 or 10 days later, depending on the experiment. Kidneys were either fixed in 4% paraformaldehyde for histological analysis or snap frozen for immunofluorescence.

Transmission electron microscopy. Samples were fixed/perfused with a 0.05% glutaraldehyde solution, embedded in Epon-812, cut in thin sections (600–900 nm), and stained with Reynolds lead citrate. Electron microscopy images were acquired under a Philips Tecnai-12 electron microscope (Philips, Eindhoven, The Netherlands).

Mouse glomeruli morphometric analysis. Morphometric analysis of glomeruli of mice after NS and PAN-induced glomerulonephritis was performed using the software ImageJ [National Institutes of Health (NIH), Bethesda, MD; http://rsb.info.nih.gov/ij/]. Whole kidneys stained with hematoxylin and eosin (H&E) were imaged using Zeiss Axioscan Z1 microscope. Glomerular occlusion was determined by measuring the ratio of patent capillary area over total glomerular area examined. Electron microscopy images were used to quantify the extent of podocyte foot process effacement and the proportion of stressed endothelial cells. Podocyte foot process effacement was expressed as proportion of the length of basal membrane covered by two or more consecutive effaced foot processes over total linear length examined. Stressed endothe-

Fig. 1. Glomeruli of diacylglycerol kinase-ε (*Dgke*) knockout (KO) mice have submicroscopic signs of endothelial impairment that worsen with age. *A*: representative light microscopy images of *Dgke* KO mice glomeruli compared with wild-type (WT) littermates at 6 wk of age. *Dgke* KO glomeruli are apparently normal and indistinguishable from WT controls. Hematoxylin and eosin (H&E), scale bars = 20 μm. *B*: on transmission electron microscopy (TEM), in the glomeruli of *Dgke* KOs, some capillaries show modest signs of endothelial stress with loss of fenestrae and swelling of the endothelial rim (black arrowheads; *left*). Segments of the glomerular basal membranes (GBMs) appear inspissated (black arrow, *left*) or duplicated for the interposition of appendices of mesangial cells (white arrows, *left* and *inset*). The epithelial compartment is relatively well preserved, and only minimal podocyte foot process effacement is observed (white arrowheads, *left* and *inset*). Notice the presence of fenestrae (black arrowheads, *right*) and the normal foot processes (white arrowheads, *right* and *inset*) in a WT littermate. Scale bars = 5 μm. *Insets* show boxed areas at higher magnification. *C*: quantification of the number of stressed endothelial cells per number of capillary loops examined. Values are means ± SE; $n = 20$ consecutive capillary loops form multiple glomeruli, with 2 mice per experimental group. *D*: urinary albumin-to-creatinine ratio (ACR) in 24-h urine of *Dgke* KO and WT mice. Values are means ± SE; $n = 3$ mice per group. ns, Nonsignificant. *E*: light microscopy images of *Dgke* KO mice glomeruli compared with WT littermates at 1 yr of age. Glomerular congestion and focal capillary obliteration (arrows) with thickening of the GBM (arrowheads) are detectable in some glomeruli of *Dgke* KOs compared with WT controls. Scale bars = 20 μm. *Insets* show boxed areas at higher magnification. *F*: TEM images of *Dgke* KO mice glomeruli compared with WT littermates at 1 yr of age. Swelling of the endothelial rim (black arrowheads) is frequently accompanied by mesangial interposition (white asterisks) and splitting of the basal membrane (white arrowhead), which are indicative of chronic glomerular repair. Scale bars = 1 μm. *G*: quantification of the number of stressed endothelial cells per number of capillary loops examined. Values are means ± SE; $n = 20$ consecutive capillary loops form multiple glomeruli, with 2 mice per experimental group. *H*: urinary ACR in 24-h urine of *Dgke* KO and WT mice. Values are means ± SE; $n = 3$ WT and 3 $Dgke^{-/-}$ mice. *P* values were calculated by Student's *t*-test.

lial cells (swollen cells with nuclei occluding more than 50% of the capillary lumen or with clear signs of endotheliosis) were manually detected in 20 consecutive capillary loops from multiple glomeruli. Results were expressed as proportion of stressed cells per number of examined capillary loops.

Immunofluorescence microscopy. The following antibodies were used: Alexa Fluor 488 conjugate goat anti-rat IgG (Invitrogen, A-11006), C3 (Abcam, ab11862) PECAM-1/CD31 (BD Biosciences, 553930), fibrin (Dako, a0080), and WT-1 (Santa Cruz, sc-7385). After standard preparation, tissues were incubated overnight at 4°C in primary antibody and for 1 h at room temperature with the fluorescently labeled secondary antibody and mounted. Images were acquired using a Zeiss Axioplan 2 deconvolution microscope or a Zeiss LSM 510 confocal microscope.

Lentiviral infection, shRNA-mediated gene silencing. Human umbilical vein epithelial cells (HUVECs) were obtained by American Type Culture Collection (Manassas, VA). *DGKE* and green fluorescent protein (GFP)-targeting short hairpin RNA (shRNA) lentiviral constructs were purchased by Open Biosystems (Lafayette, CO). The experiments were performed as previously described (21).

Wound-healing test for endothelial cell migration. HUVECs were plated on glass-bottomed cells for 48 h to allow them to reach full confluence. A wound in the monolayer was then created by scratching the cells with a pipette tip, and images were taken 6 h later using a Zeiss LSM 510 microscope at four different points along the wound. Migration quantification was performed using the software ImageJ (NIH, Bethesda, MD; http://rsb.info.nih.gov/ij/) and was expressed as a percentage of the distance covered by migrating cells over the initial distance between the edges of the wound. PGE_2 was purchased by Cayman Chemicals (Ann Arbor, MI) and was used at a final concentration of 3 μM.

In vivo angiogenesis assay. The subcutaneous sponge model was used to determine the effects of prostanoids on in vivo angiogenesis (34). Sterile polyvinyl-acetal CF-50 round sponges (6-mm diameter, 50-μm pores, Medtronic Xomed) were implanted under the flank skin of wild-type and *Dgke* knockout mice (10 wk of age, 25 g body wt, $n = 3$ per treatment). The sponges were then injected on alternate days with 50 μl of either vehicle phosphate buffer saline (PBS) or PGE_2 (10 μM). After 14 days, the sponges were isolated and snap frozen for immunofluorescence, which was performed on a Zeiss LSM 510 Meta Confocal Microscope. The area and the number of PECAM-1/CD31 positive structures were quantified by digital image analysis of 10 random images per sponge (total of 30 images per treatment group) using the software ImageJ (NIH, Bethesda, MD, http://rsb.info.nih.gov/ij/).

Macrophages isolation and culture. Bone marrow macrophage precursors were isolated as described elsewhere (Nature Lipidomics Gateway, protocol ID: PP0000003500).

Isolation of mouse glomeruli. Mice were perfused with 8×10^7 Dynabeds (Invitrogen, Carlsbad, CA) in 40 ml of Hanks' balanced salt solution. Kidneys were minced into 1-mm^3 pieces and incubated with collagenase A (1 mg/ml) and DNAse I (1 U/ml) at 37°C for 30 min with gentle agitation. Collagenase-digested tissues were sequentially pressed through a cell strainer at 4°C, washed three times in Hanks' balanced salt solution, and collected with a Magnetic Particle Concentrator.

Quantitative real-time PCR. Total RNA was isolated using TRIzol (Invitrogen, Carlsbad, CA) and purified with Qiagen RNeasy Mini Kit, according to the manufacturer's protocols. First-strand reverse transcription reactions were performed using the ThermoScript RT-PCR Kit (Invitrogen). Real-time PCR were performed using iQ SYBR Green Supermix (Bio-Rad). The *β-actin* gene was used as a normalizer.

Measurement of serum creatinine and blood urea nitrogen. Serum creatinine concentrations were determined by capillary electrophoresis at the physiology core of O'Brien Center for Kidney Diseases in Dallas, TX. Blood urea nitrogen measurements were obtained using the Vitrops 250 chemistry analyzer.

Measurement of urinary albumin and creatinine. Twenty-four-hour urine was collected using metabolic cages. Urinary albumin concentration was determined using the Albuwell microalbumin ELISA essay (Exocell, Philadelphia, PA). Urinary creatinine concentration was determined using a P/ACE MDQ Capillary Electrophoresis System and photodiode detector (Beckman-Coulter, Fullerton, CA) at 214 nm (44) in the physiology core of the O'Brien Center for Kidney Diseases in Dallas. Urinary albumin concentrations were normalized to the amount of excreted creatinine.

Measurement of urinary prostanoids. Prostanoids were extracted by solid phase chromatography using octadecyl silica cartridges, resuspended in 25 μl of 70:30 methanol/water solution, and subjected to triple-quadruple (Waters, TQ-S) electrospray tandem mass spectrometry after adding an internal standard (Cayman Biochemicals, Ann Arbor, MI) for quantification. Urinary prostanoid concentrations were normalized to milligrams of excreted creatinine.

Statistical analysis. Data analysis was performed using Excel (Microsoft) and Prism (version 5.03) software (GraphPad Software, San Diego, CA). Data are presented as means ± SE, unless otherwise specified. Two-tailed unpaired Student's *t*-test or nonparametric Mann-Whitney test were used to compare two groups of data.

RESULTS

Glomeruli of Dgke knockout mice have submicroscopic signs of endothelial impairment that become more pronounced with age. *Dgke* knockout mice, which were previously generated to study the contribution of arachidonate signaling to epileptogenesis, are fertile and do not present any apparent phenotype (36). $Dgke^{-/-}$ light microscopy examination of H&E sections of *Dgke* knockout kidneys between 4 and 6 wk of age did not show significant differences, compared with wild-type littermates (Fig. 1*A*). Careful examination of transmission electron microscopy (TEM) images of *Dgke* knockout glomeruli, instead, evidenced modest signs of endothelial stress that were not detected in wild-type mice (Fig. 1, *B* and *C*): some endothelial cells in $Dgke^{-/-}$ glomeruli lost the normal fenestrated appearance and presented swelling of the endothelial rim. Segments of the GBMs were also abnormally inspissated or duplicated for the interposition of mesangial cells appendices, whereas the epithelial compartment was relatively well preserved, but no significant differences in albuminuria were detected between knockout and wild-type mice (Fig. 1*D*). The glomerular lesions became more severe in *Dgke*

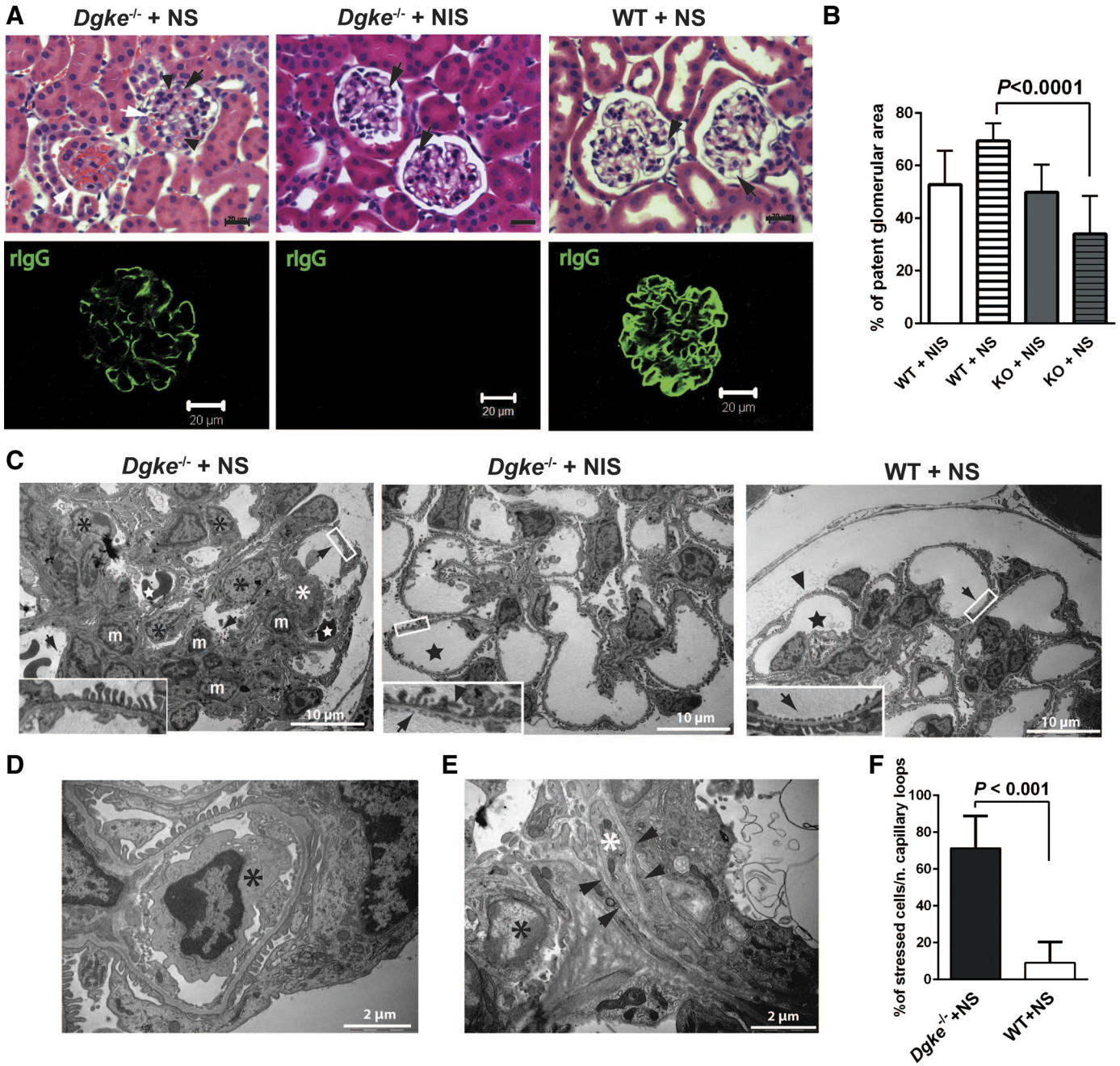

Fig. 2. *Dgke* KO mice develop glomerular thrombotic microangiopathy when injected with nephrotoxic serum (NS). *A*: representative images of *Dgke* KO mice glomeruli (*left*) after injection of subtoxic doses of rabbit NS compared with WT littermates (*right*). Glomeruli of KO mice show increased mesangial matrix (arrowheads), diffuse congestion of the capillary loops (black arrow), and numerous entrapped erythrocytes (white arrow). Capillary obliteration is not detectable in WT littermates (*right*) after injection of the same dose of NS (arrows indicate patent capillary loops) and in *Dgke* KOs treated with nonimmune isotypic serum (NIS; *center*). H&E staining, scale bars = 20 μm. *Bottom*: immunofluorescence microscopy images of glomeruli of the same mice probed with an antibody against rabbit IgG (rIgG), showing that the animals received comparable amount of NS or no NS in the NIS control. Mice were 6 wk of age at the date of the experiment. Scale bars = 20 μm. *B*: quantification of the average patent capillary area in glomeruli of WT and *Dgke* KO mice after injection of NS or of isotypic NIS as a control, obtained by digital image analysis. Values are means ± SE; $n = 2$ mice per group, with 10 optical fields per mouse. *P* values were calculated by Student's *t*-test. *C*: TEM images of *Dgke* KO after NS or isotypic NIS injections and WT littermate glomeruli after NS injection. In kidneys of *Dgke* KOs after NS injection (*left*) mesangial cells (m) are focally increased in number and infiltrate segments of the GBM (white asterisk). Endothelial cells (black asterisks) are swollen, and capillary rims are irregular and lack the typical fenestrations (black arrows). Lumens are partially obliterated by swollen endothelium and trapped irregular-shaped erythrocytes (stars). Notice that podocytes' foot processes (black arrowhead and *inset*) are relatively well conserved. Capillary loops of *Dgke* KOs treated with NIS and of WT littermates after NS injections (stars; *middle* and *right*) are patent, endothelial fenestrations are clearly detectable (arrows and *insets*), and podocytes' foot processes appear normal (arrowhead). Scale bars = 10 μm. *D* and *E*: TEM images at higher magnification of *Dgke* KO glomeruli after injection of NS that show bulky endothelial cells (black asterisks) with almost completely obstructed capillary lumens and the interposition of a mesangial cell (*E*; white asterisk), which results in the splitting of the basal membrane (*E*; black arrowheads). Scale bars = 2 μm. *F*: quantification of the number of stressed endothelial cells per number of capillary loops in glomeruli of *Dgke* KO and WT mice 14 days after injection with NS. Values are means ± SE; $n = 20$ consecutive capillary loops form multiple glomeruli, with 2 mice per experimental group.

knockout mice at 1 yr of age: in H&E kidney sections, glomeruli had more frequently the typical "avascular" appearance, focal thickening of the capillary walls, and prominent endothelial cells nuclei (Fig. 1*E*). By TEM, signs of important endotheliosis, mesangial interposition, and splitting of the basal membrane were also evident (Fig. 1, *F* and *G*), recapitulating the glomerular human pathology of subjects with *DGKE* loss of function mutations. Urinary albumin tended to be higher in *Dgke* knockout mice compared with wild-type controls (Fig. 1*H*).

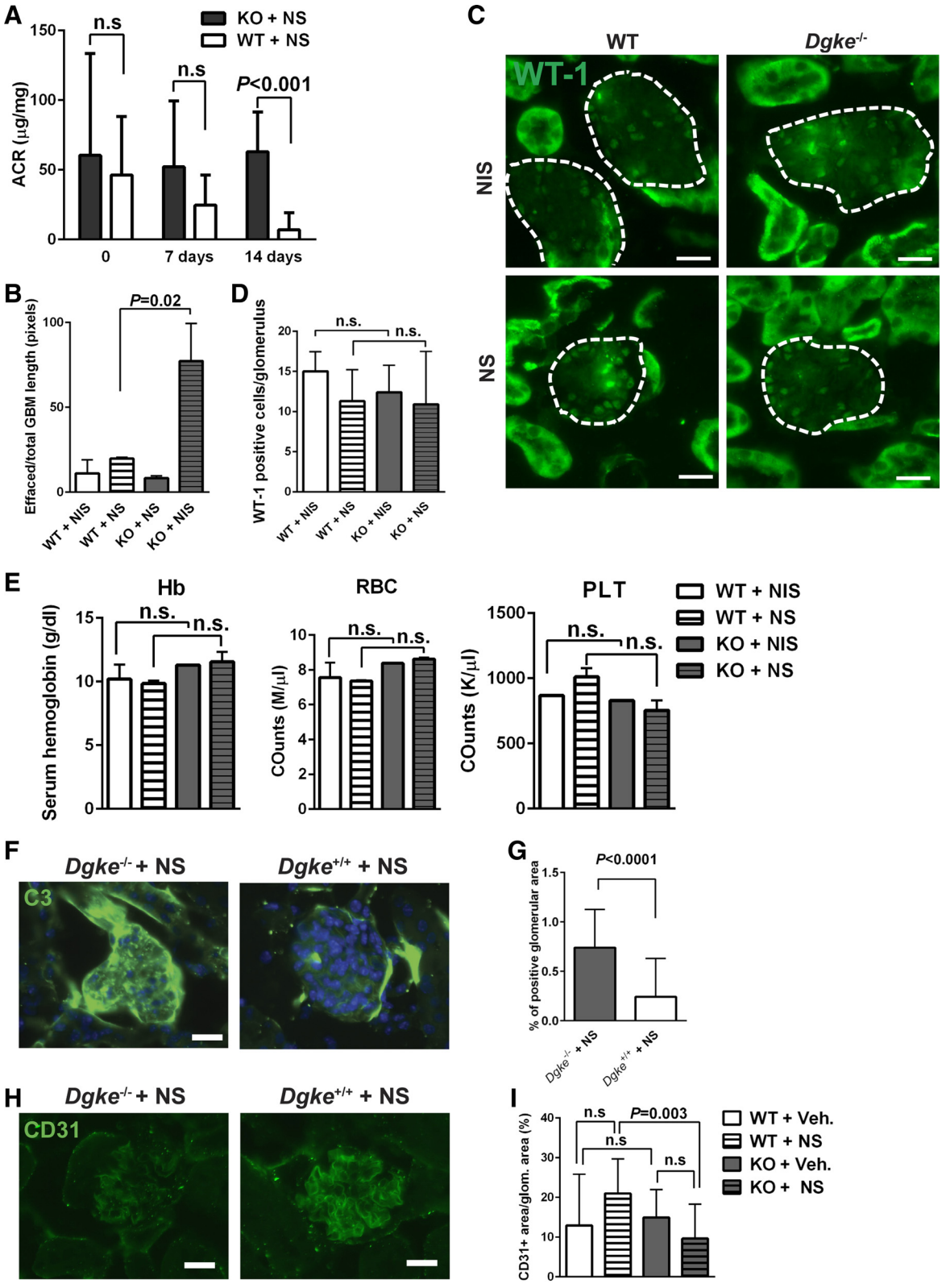

Dgke knockout mice are more susceptible to glomerular injury when challenged with NS. To determine if *Dgke* knockouts were more exposed of wild-type mice to develop acute phenotype at younger age, we used an experimental model of immune-mediated glomerulonephritis, challenging the mice with NS (10, 43). To this purpose, we injected 4-wk-old *Dgke* knockouts and wild-type littermates with Freund's adjuvant, followed, after 5 days, by the injection of subtoxic doses of NS or NIS as a control. The mice were killed 14 days later, and kidneys were examined by light and electron microscopy. H&E sections of kidneys of *Dgke* knockout mice that received NS had evident signs of microvascular congestion: capillary loops, were partially or completely obliterated, and trapped erythrocytes were frequently observed. Hypercellularity and mesangial expansion were also evident (Fig. 2, *A*, *top left*, and *B*). Oppositely, $Dgke^{+/+}$ mice challenged with NS (Fig. 2, *A*, *top right*, and *B*) and *Dgke* knockout mice that received NIS (Fig. 2, *A*, *top middle*, and *B*) appeared mostly normal, showing normocellular glomeruli and patent capillary tufts. Similarly, TEM of glomeruli of $Dgke^{-/-}$ mice treated with NS (Fig. 2, *C*, *left*, and *F*) presented mesangial expansion and infiltration of the GBM, loss of endothelial fenestrae, diffuse swelling of the endothelial cells that partially obliterated the capillary lumens, and trapped erythrocytes. Instead, capillary loops of *Dgke* knockout mice treated with NIS and of wild-type littermates' glomeruli after NS (Fig. 2, *C*, *center* and *right*, and *F*) were patent with clearly detectable endothelial fenestrations. *Dgke* knockout mice had higher levels of urinary albumin (Fig. 3*A*) and more diffuse foot process effacement (Fig. 3*B*) 14 days after NS injection, suggesting impaired repairing capacity after immune-mediated glomerular injury. No significant differences were detected in the number of glomerular podocytes (Fig. 3, *C* and *D*) and in serum hemoglobin, red blood cells, and platelet counts among all of the experimental groups (Fig. 3*E*). On immunofluorescence microscopy, glomeruli of *Dgke* knockout mice treated with NS were more often positive for complement C3 (Fig. 3, *F* and *G*) and expressed less anti-thrombotic PECAM-1 (CD31 in the figures, Fig. 3, *H* and *I*), compared with wild-type NS-treated controls. These data indicate that lack of *Dgke* predisposes to extensive glomerular capillary occlusion after immunomediated glomerular injury.

Dgke knockout mice are resistant to PAN-induced glomerulonephritis. The model of immune-mediated nephritis used in the previous experiment is based on complement activation that is triggered by the deposition of antibodies raised against GBM antigens. To test if *Dgke* knockout mice are more susceptible also to IgG/complement-independent glomerular injury, we treated mice with PAN, a drug with selective podocyte toxicity that induces self-limited damage, independent from complement activation (16). *Dgke* knockouts and wild-type littermates between 8 and 10 wk of age were injected with PAN (0.5 $mg \cdot g^{-1} \cdot day^{-1}$ for 2 days), and kidney histology was evaluated after 3 days, when the highest acute PAN toxicity has been reported (2), and 10 days, to monitor recovery from injury. By light microscopy of H&E-stained kidney sections, we observed congestion in some glomeruli of *Dgke* knockout and wild-type mice treated with PAN (Fig. 4*A*), but no statistically significant difference was detected between these two groups (Fig. 4*B*, 150 glomeruli examined, 50 random chosen glomeruli per mouse, 3 mice per group). In TEM images (Fig. 4*C*), some glomeruli of knockout and wild-type mice treated with PAN showed signs of mild endothelial stress (swollen endothelial cells with enlarged nuclei, absence of capillary fenestrations, and blebs of the endothelial rim), whereas podocytes' foot processes were often well conserved. Conversely, podocytes' foot processes in wild-type mice treated with PAN were extensively effaced, as shown by morphometric analysis of foot process effacement of TEM images (Fig. 4*D*, 10 glomeruli per mouse, $n = 4$ mice per group). Consistent with this finding, urinary albumin-to-creatinine ratios from 24-h urine collections were lower in *Dgke* knockouts after PAN injection compared with wild-type controls 3 days after treatment, and recovered faster by *day 10* (Fig. 4*E*). No differences in the number of podocytes were detected between the experimental groups (Fig. 4*F*). By immunofluorescence microscopy, we detected complement C3 in a single glomerulus in one *Dgke* knockout (Fig. 4*G*, arrow) but never in wild-type mice (50 glomeruli counted per mouse, $n = 3$ mice per group). We conclude that, at the used doses, PAN induces mild endotheliosis in both *Dgke* knockout and wild-type mice, and that *Dgke* knockout podocytes are more resistant to PAN injury compared with wild-type controls.

Dgke is required for the expression of the inducible enzyme Cox-2 in normal glomeruli. Cox-2 is a ubiquitous enzyme required for a rate-limiting reaction in the synthesis of PGs from AA. Unlike the cognate enzyme Cox-1 that is constitutively active, Cox-2 is an inducible enzyme (33, 38). In the kidney, Cox-2 is expressed in glomeruli, thick ascending limb of Henle, and in medullary interstitial cells (14). Importantly, *Cox-2* is expressed by podocytes, and it is required for correct glomerular homeostasis (3, 13): both increased and decreased *Cox-2* expression in mouse podo-

Fig. 3. Morphometric and functional analysis of *Dgke* KO mice after NS injury. *A*: albumin concentrations in 24-h urine collected from *Dgke* KO and WT mice in basal conditions and at 7 and 14 days after injection with NS or NIS, a control. Values are means ± SE. $n = 3$ WT and 3 *Dgke* KO mice per group. *P* values were calculated by Student's *t*-test. *B*: average length of podocyte effacement calculated by digital image analysis of TEM images. Values are means ± SD; $n = 10$ images per mouse, with 2 mice per experimental group. *P* values were calculated by Student's *t*-test. Immunofluorescence microscopy images (*C*) and quantification (*D*) of the number of WT-1-positive podocytes per glomerulus in the four experimental groups are shown. Values are means ± SD; $n = 3$ mice per group. *E*: serum hemoglobin (Hb), red blood cells (RBC), and platelet (PLT) count in *Dgke* KO and WT mice in basal conditions and at 14 days after injection with NS or NIS, a control. No significant difference among these parameters was detected. Values are means ± SD; $n = 3$ mice per group. *P* values were ns, calculated by Student's *t*-test. *F*: representative immunofluorescence microscopy images *Dgke* KO mice glomeruli (*left*) after NS injection compared with WT littermates (*right*), using an antibody against the complement C3. *G*: quantification of the number of glomeruli positive for C3 deposition. Values are means ± SE; $n = 2$ mice per group, with 20 glomeruli per mouse. *P* values were calculated by Student's *t*-test. *H* and *I*: representative immunofluorescence microscopy images (*H*) and digital quantification (*I*) of glomerular CD31 expression in *Dgke* KO kidneys and WT mice 14 days after treatment with NS or with NIS as a control. Veh, vehicle.

cytes, in fact, result in different forms of glomerular disease, indicating that a balanced activity of this enzyme is necessary for correct glomerular development and maintenance (3). Microarray expression analysis of mouse brains after electrical shock had previously revealed that *Dgke* knockouts failed to induce transcription of *Cox-2* compared with wild-type controls (22). We tested if Cox-2 expression after stress was also compromised in other tissues and more specifically in kidneys. Since *Cox-2* expression is induced in macrophages (39) and fibroblasts (5) when stimulated with lipopolysaccharide (LPS) and with interleukin 1β (IL-1β), respectively, we measured by quantitative real-time PCR the levels of *Cox-2* mRNA in $Dgke^{-/-}$ and wild-type bone marrow-derived macrophage precursors, 12 h after stimulation with LPS (4 ng/ml) and in skin primary fibroblasts cultured for 4 h in medium supplemented with IL-1β (2 ng/μl). We found that expression of *Cox-2* was upregulated after exposure to LPS in wild-type bone marrow-derived

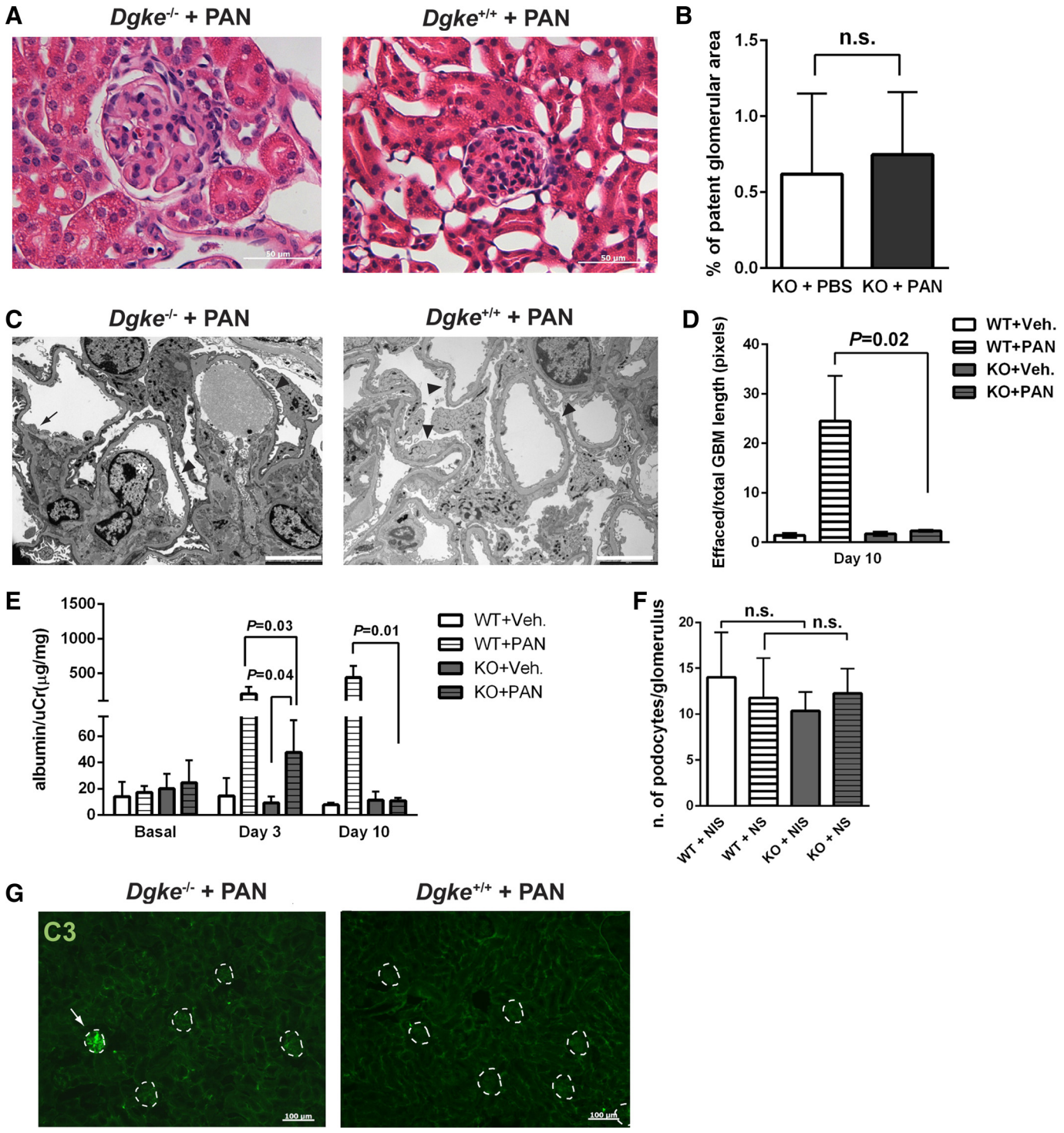

macrophage precursors (Fig. 5*A*), but not in *Dgke*$^{-/-}$ cells, and in wild-type, but not in knockout fibroblasts, exposed to IL-1β (Fig. 5*B*). Western blots of fibroblasts extracts confirmed the impaired expression of Cox-2 in *Dgke* null cells, both in basal conditions and after IL-1β stimulation (Fig. 5*C*). No changes in *Cox-1* expression in wild-type and knockout fibroblasts were detected by quantitative real-time PCR and Western blot (not shown). Then we asked if *Cox-2* induction is also compromised in *Dgke* knockout kidneys. We examined by quantitative real-time PCR and by Western blot cortex extracts 3 days after injections with PAN or vehicle-injected controls. *Cox-2* transcripts were similar in *Dgke* knockouts and in wild-type littermates, but failed to be upregulated after PAN injection (Fig. 5*D*). Similarly, Cox-2 protein levels were reduced in cortexes from *Dgke* knockout mice after PAN injection compared with wild-type littermates (Fig. 5*E*). Importantly, *Cox-2* expression was also impaired in *Dgke*$^{-/-}$ isolated glomeruli (Fig. 5*F*). The lower expression levels of Cox-2 in *Dgke* null glomeruli compared with wild type is consistent with the reduced proteinuria and podocytes foot process effacement observed in *Dgke* knockout mice, in agreement with the detrimental effect of Cox-2 on these parameters (3, 4, 40).

Lack of Dgke affects prostanoid synthesis in mouse kidneys. Cox-2 and the cognate enzyme Cox-1 catalyze the formation of the cyclic endoperoxides PGG_2 and PGH_2, which are obligate intermediates for the synthesis of prostanoids. Although Cox-2 and Cox-1 potentially act on the same substrate, they have a different affinity for AA and are functionally coupled with different prostanoid synthases (27). As a consequence, PGE_2 and PGF_2 synthesis in the kidney is mostly dependent on Cox-2 activity (33). PGE_2 is the most abundant prostanoid in the kidney and has multiple effects on the glomerular circulation, acting as a vasodilator of the afferent arteriole and modulating the constrictor effect of angiotensin II on mesangial cells (7, 37). PGE_2 is also capable to promote proliferation and migration of HUVEC cells in vitro and to sustain angiogenesis in vivo (28, 34). For this reason, we measured the levels of PGE_2 and $PGF_{2\alpha}$ in the urine of *Dgke*$^{-/-}$ mice and wild-type littermates, 3 days after PAN injection, by liquid chromatography-electrospray tandem mass spectrometry (23). Concordant with Cox-2 expression, the urinary excretion of these two Cox-2 enzymatic products was reduced in *Dgke*$^{-/-}$ mice compared with wild-type controls after PAN injection (Fig. 6), indicating impaired induction of prostanoid synthesis in *Dgke* null mice after podocyte stress. Twenty-four-hour urinary 11-dehydrothromboxane B_2, the degradation product of TxA_2, was also lower in knockout mice after PAN injection compared with the wild type, although the difference did not reach statistical significance.

Dgke knockout endothelial cells present defects that improve with PGE_2 supplementation. Recently, loss of *Dgke* has been associated with impaired motility and angiogenesis, distress of endothelial cells, and increased apoptosis in vitro, suggesting a cell-autonomous endothelial function of *Dgke* (1). Given the important pro-angiogenic effect of PGE_2 on endothelial cells (1, 34), we hypothesized that impaired PGE_2 production in *Dgke* knockout mice may concur to the endothelial stress observed in the absence of *Dgke*. Activated endothelial cells express more pro-thrombotic factors, such as intercellular adhesion molecule-1 and tissue factor, and less anti-thrombotic molecules, such as PECAM-1. PECAM-1 is a cell-cell junction protein that is important for normal angiogenesis (6) and is known to inhibit thrombus formation in vivo (8). To test the expression of this protein in *Dgke* knockout glomeruli, we probed wild-type and *Dgke* knockout kidneys treated either with PAN or vehicle, with an antibody against PECAM-1. Digital analysis of immunofluorescence microscopy images showed that glomeruli of knockout mice after PAN had reduced PECAM-1 expression, compared with wild-type mice (Fig. 7, *A* and *B*). Expression of PECAM-1 was also impaired in cortexes of *Dgke* knockout mice in basal conditions and 3 days after PAN injection, as detected by quantitative real-time PCR (Fig. 7*C*). To verify if PGE_2 may affect PECAM-1 expression in *Dgke* defective endothelial cells, we silenced *DGKE* in HUVEC cells by shRNA and estimated the amount of PECAM-1 by Western blot after exposing these cells to PGE_2 for 4 h. We found that PECAM-1 protein levels were lower in HUVEC cells after *DGKE* silencing compared with the GFP-silenced controls. The amount of PECAM-1 increased, though, after exposing HUVECs to PGE_2-supplemented medium, indicating that PGE_2 is required to induce PECAM expression in HUVECs (Fig. 7*D*). We asked, then, if PGE_2 supplementation could also improve the migration defects presented by the *DGKE* knockdown HUVECs in vitro (1). To this purpose, we assayed the effect of PGE_2 on migratory ability of *DGKE* knockdown HUVEC cells in a wound-healing assay in vitro, by measuring the migration of *DGKE* knockdown cells on a coverslip after scratching the cell monolayer with a pipette tip. The distance covered by migrating cells after wounding was lower in *DGKE* knockdown cells compared with GFP-targeted controls, as previously described

Fig. 4. Puromycin aminonucleoside (PAN)-induced glomerulonephritis in *Dgke* KO mice promotes glomerular endothelial lesions in the absence of significant complement activation. *A*: light microscopy images of *Dgke* KO mice glomeruli (*left*) and WT littermate (*right*) 3 days after PAN injections. The capillary spaces in some glomeruli of both *Dgke* KO and WT mice after PAN injection are occluded. *B*: quantification of the average patent capillary area in glomeruli of WT and *Dgke* KO mice after PAN injection, obtained by digital image analysis. Values are means ± SD; $n = 3$ mice per group, with 10 optical fields per mouse. *P* values were calculated by Student's *t*-test. *C*: TEM images of a glomerulus of a *Dgke* KO mouse (*left*) and a WT littermate (*right*) 3 days after PAN injection. Some endothelial cells are swollen and have enlarged nuclei (white asterisk), and some capillaries present loss of endothelial fenestrations (black arrow). Podocytes' foot processes are often conserved in *Dgke* KO mice treated with PAN (*left*; arrowheads) and more extensively effaced in WT mice treated with PAN (*right*; arrowheads). Scale bars = 5 μm. *D*: average length of podocyte effacement calculated by digital image analysis of TEM images. Values are means ± SD; $n = 10$ images per mouse, with 4 mice per experimental group. *P* values were calculated by Student's *t*-test. *E*: 24-h urinary ACR of *Dgke*$^{-/-}$ and WT mice treated with PAN or Veh as a control. *Dgke* KO mice are partially protected from developing acute proteinuria and recover faster after PAN treatment, compared with WT controls. Values are means ± SD; $n = 4$ mice per experimental group. *P* values were calculated by Student's *t*-test. *F*: quantification of the number of podocytes per glomerulus in the 4 experimental groups, obtained by morphological analysis of TEM images. Values are means ± SD; $n = 5$ glomeruli per mouse, with 3 mice per group. *P* values were calculated by Student's *t*-test. *G*: immunofluorescence microscopy images of complement C3 deposition in glomeruli of *Dgke* KO mice and WT controls 10 days after PAN injection. Glomeruli are highlighted by a dashed line. One single glomerulus was positive in a *Dgke* KO mouse (arrow). $n = 50$ glomeruli counted per mouse, 3 mice per group. Scale bars = 100 μm.

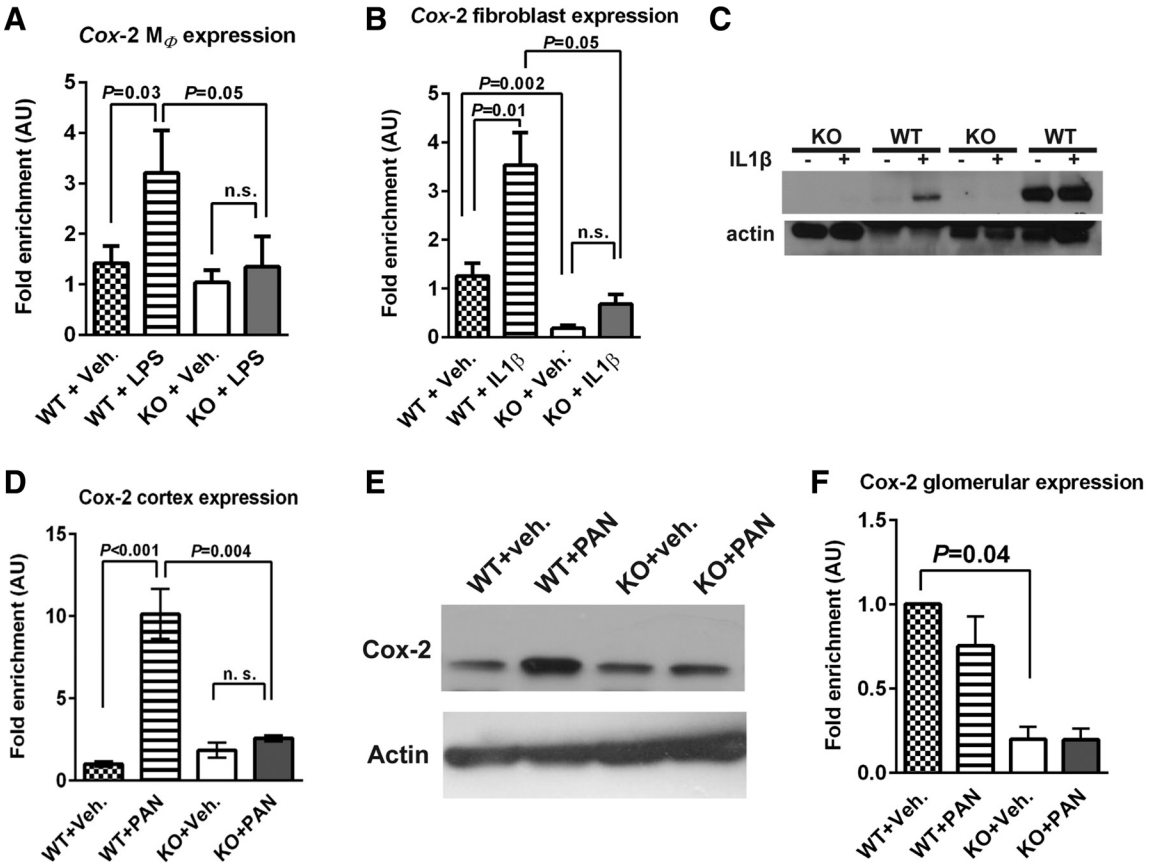

Fig. 5. Cyclooxygenase-2 (*Cox-2*) induction is impaired in *Dgke* null cells. *A*: quantification of *Cox-2* expression, measured by real-time PCR, in bone marrow-derived macrophage ($M\Phi$) precursors, isolated from *Dgke* KO mice and WT littermates and exposed to LPS or Veh as a control. *Cox-2* expression is induced by stimulation with LPS in $M\Phi$ isolated from WT but not from *Dgke* KOs ($n = 6$ mice per group). AU, arbitrary units. Values are means ± SE. *P* values were calculated by Student's *t*-test. *B*: quantification by real-time PCR of *Dgke* KO and WT skin fibroblasts stimulated with IL-1β. *Cox-2* expression is decreased in mutant fibroblasts and fails to be induced after IL-1β stimulation. Values are means ± SE; $n = 4$ mice per group. *P* values were calculated by Student's *t*-test. *C*: Western blot of *Dgke* KO and WT fibroblast lysates exposed to IL-1β or Veh as a control, probed with an antibody against *Cox-2*. Two replicates were loaded for each experimental condition. *Cox-2* was undetectable in *Dgke* KO fibroblasts before and after stimulation with IL-1β, but was abundantly expressed in WT cells. For two WT samples (*column 3* and *4* from *left*), one-half of the amount of protein was loaded to show the increase of *Cox-2* expression after exposure to IL-1β. *D*: quantification by real-time PCR of the transcripts of *Cox-2* in kidney cortexes of *Dgke* KO mice and WT littermates, 3 days after the injection of PAN or Veh as a control. *Cox-2* expression in *Dgke* KO cortexes is increased in PAN-treated WT mice, but not in *Dgke* KOs. Values are means ± SE; $n = 4$ mice per group. *P* values were calculated by Student's *t*-test. *E*: Western blot showing the amount of *Cox-2* in in kidney cortexes of *Dgke* KO mice and WT controls, 3 days after treatment with PAN or Veh as a control. *Cox-2* is increased in cortexes of PAN-treated WT mice, but not in *Dgke* KOs. *F*: quantification by real-time PCR of *Cox-2* expression in isolated glomeruli from *Dgke* KO mice and WT littermates, 3 days after the injection of PAN or Veh as a control. *Cox-2* expression in *Dgke* KO glomeruli is induced in PAN-treated WT mice, but not in *Dgke* KOs. Values are means ± SE; $n = 4$ mice per group. *P* values were calculated by Student's *t*-test.

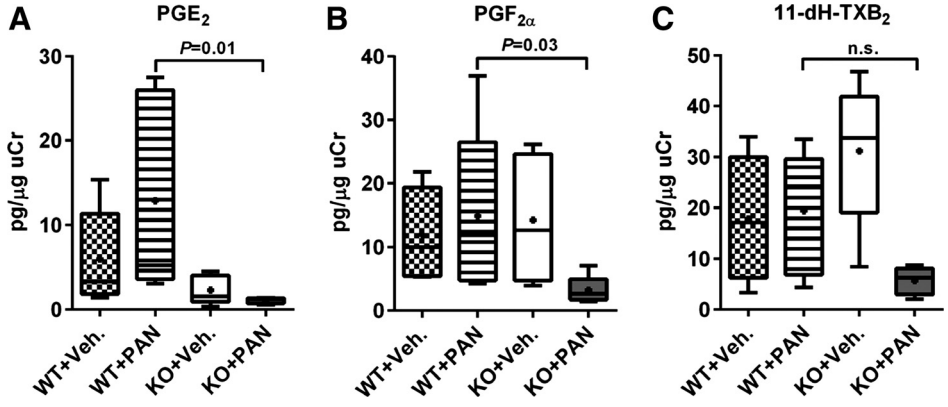

Fig. 6. Lack of Dgke affects prostanoids synthesis in mouse kidneys. Urinary concentrations of prostaglandins (PG) E_2 (*A*), PGF_2 (*B*), and 11-dehydrothromboxane B_2 (11-dh-TxB_2; *C*) in 24-h urine of *Dgke* KOs and WT controls in basal conditions and 3 days after PAN injection or Veh as a control, determined by liquid chromatography-electrospray tandem mass spectrometry. Excretion is significantly lower in *Dgke* KOs compared with controls after PAN treatment. Box and whiskers are 25th and 75th and minimum and maximum, respectively. Lines represent medians; dots correspond to means. Values are means ± SE; $n = 4$ samples per group. *P* values were calculated with the Mann-Whitney rank sum *t*-test. uCr, urinary creatinine.

(1), but improved with PGE_2 supplementation (Fig. 7, *E* and *F*). Finally, to explore if PGE_2 supplementation may affect endothelial angiogenesis also in vivo, we performed experiments of angiogenesis in subcutaneous sponge implants (1, 32). Sterile polyvinyl-acetal sponges were implanted under the flank skin of *Dgke* knockout mice and of wild-type littermates (8–12 wk of age, $n = 4$ mice) and were injected with PGE_2 or with equal volume of PBS, on alternate days for 14 days. After this time, mice were killed, and sponges were collected, fixed with paraformaldehyde, and probed with an antibody against PECAM-1. Images were taken by immunofluorescence confocal microscopy, and the extent of PECAM-1-positive surface or the number of positive neovascularized structures per random microscopy field was quantified by digital image analysis. We found that sponges implanted in *Dgke* knockout mice had reduced PECAM-1-positive structures and reduced average PECAM-1-positive surface per neovascularized structure, compared with sponges implanted in wild-type littermates (Fig. 7, *G–I*, $n = 2$ sponges per mouse in each group, 4 mice per group). Importantly, expression of PECAM-1 increased in sponges injected with PGE_2, suggesting that the defective angiogenic potential of *Dgke* null endothelial cells may be partially reversed by PGE_2.

DISCUSSION

In the present work, we have characterized the glomerular phenotype of *Dgke* knockout mice and investigated possible mechanisms of disease promoted by lack of *Dgke*. $Dgke^{-/-}$ mice are more resistant than wild type to develop seizures after brain electrical stimulation, but no apparent kidney phenotype has been so far reported (36). Here we have shown that, although *Dgke* null mice do not have spontaneous clinical signs of kidney disease and have normal serum creatinine and urinary albumin, they present microscopic glomerular lesions (endotheliosis and mesangial interposition of the GBM) that worsen with age, and that they are more susceptible to develop overt glomerular congestion after NS injury. We also tested the susceptibility of *Dgke* knockout mice to immuno-independent glomerular injury by administering PAN, a drug with selective podocyte toxicity (16). Administration of PAN was associated with signs of endothelial stress in glomeruli of both *Dgke* knockout and wild-type mice, suggesting that these lesions are secondary to podocyte injury. We did not detect significant glomerular deposition of complement C3 between *Dgke* knockout and wild-type mice, at the used PAN dosage. Unfortunately, we were not able to perform the experiment with higher dosage or prolonged exposure to PAN, because of the high mouse mortality that we observed in these experimental conditions. However, after NS-induced nephritis, we noticed that more glomeruli were positive for complement C3 in *Dgke* knockout mice compared with controls. In the attempt to reconcile these evidences, we can speculate that complement activation is not the initial determinant of the phenotype in *Dgke* knockouts, but *Dgke* null endothelial cells may be more susceptible to fix the complement secondarily, because they are more susceptible to injury and death. This hypothesis is compatible with the recent report that *DGKE* knockdown HUVEC cells have an increased tendency to apoptosis and decreased expression of two cell surface regulators of the complement activation, the complement inhibitor membrane cofactor protein and the decay accelerating factor (1). The authors of this paper, though, failed to detect complement deposition on these cells in a test in vitro, and, therefore, more targeted in vivo studies will be required to clarify this point. Another question that will need to be addressed, which will require the use of tissue-specific *Dgke* knockouts, is if endothelial cells, podocytes, or both contribute to determine the glomerular lesions in the absence of *Dgke*. The effect of *DGKE* small interfering RNA-mediated silencing on HUVEC cell survival and angiogenic potential indicates cell-autonomous functions of *Dgke* in the endothelium. On the other hand, the impaired *Cox-2* expression after stress in all of the cell lines and tissues that we have examined, including kidney glomeruli, infers that *Dgke* is required for *Cox-2* induction also in podocytes, which is the principal glomerular source of Cox-2 (18), and may affect the defective endothelium in a cell nonautonomous fashion, through impaired production of PGE_2. This hypothesis is corroborated by our in vitro and in vivo experiments that show improved angiogenic potential and PECAM-1 expression of *DGKE* knockdown HUVEC cells after PGE_2 supplementation. The resistance of *Dgke* null podocytes to PAN injury, in fact, argues that the reduced Cox-2 expression in *Dgke* null glomeruli is not secondary to loss of podocytes. Finally, the mechanisms by which *Dgke* controls *Cox-2*

Fig. 7. *Dgke* KO mice have endothelial defects that improve with PGE_2 supplementation. *A* and *B*: representative immunofluorescence microscopy images (*A*) and quantification by digital image analysis (*B*) of glomerular CD31 expression in *Dgke* KO kidneys and WT mice 3 days after treatment with PAN or with PBS as a control. CD31 signal was lower in *Dgke* KOs compared with controls. Glomeruli are highlighted by dotted lines. Scale bars = 50 μm. Quantification data are expressed as average ± SD ($n = 3$ mice, 10 optical fields per mouse). *C*: expression of CD31 in cortexes of *Dgke* KO and WT mice, 3 days after treatment with PAN or with PBS as a control, measured by quantitative real-time PCR. Values are means ± SE from triplicate samples. *P* values were calculated by Student's *t*-test. *D*: Western blot of human umbilical vein epithelial cell (HUVEC) lysates after short hairpin RNA (shRNA)-mediated silencing of *DGKE* (sh-*Dgke*) compared with control cells infected with a green fluorescent protein (GFP)-targeting shRNA (sh-GFP). CD31 is lower in *DGKE*-silenced HUVECs compared with the controls and increases after 4-h exposure to PGE_2 supplemented medium. *E*: representative differential interference contrast microscopy images of *DGKE* knockdown and GFP-targeted control HUVECs immediately after wounding the cell monolayers (0 h) and 6 h after exposure to PGE_2-supplemented medium or to Veh-supplemented medium, as a control. Dashed lines were overlaid to the images to mark the border of the wound. *F*: quantification by digital image analysis of the distance covered by endothelial cells migrated from the border of the wound 5 h after exposure to PGE_2 supplemented medium, expressed as the ratio between covered distance and total width of the wound. Data from triplicate experiments are expressed as average ± SE. *P* values were calculated by Student's *t*-test. *G*: representative immunofluorescence confocal microscopy images of polyvinyl-acetal sponges implanted subcutaneously in *Dgke* KO mice (8–12 wk of age, $n = 4$ sponges per mouse, 4 mice) and of WT littermates injected with PGE_2 or with equal volume of Veh on alternate days for 14 days, probed with an antibody against CD31. Scale bars = 20 μm. *H* and *I*: quantification by digital image analysis of the number of positive neovascularized structures, expressed as average of CD3-immunoreactive area of CD31-positive structures (*H*), or as number of CD31-positive structures per random microscopy field (*I*). Data were obtained analyzing 10 random images per sponge and are expressed as average ± SD; $n = 4$ sponges per mouse, with 4 mice per each experimental group. *P* values were calculated by Student's *t*-test.

induction will also need to be investigated. Dgkε is required to maintain the phospholipids acyl composition of the cell membranes, and thus is likely to affect multiple downstream signaling pathways. If and how any of these pathways may regulate Cox-2 expression will need to be experimentally proved. In summary, we have reported that *Dgke* knockout mice have glomerular pathology that reproduces the lesions observed in patients with biallelic loss of function mutations in *DGKE*. Our studies also show that the lipid kinase Dgkε is required for the maintenance of the glomerular endothe-

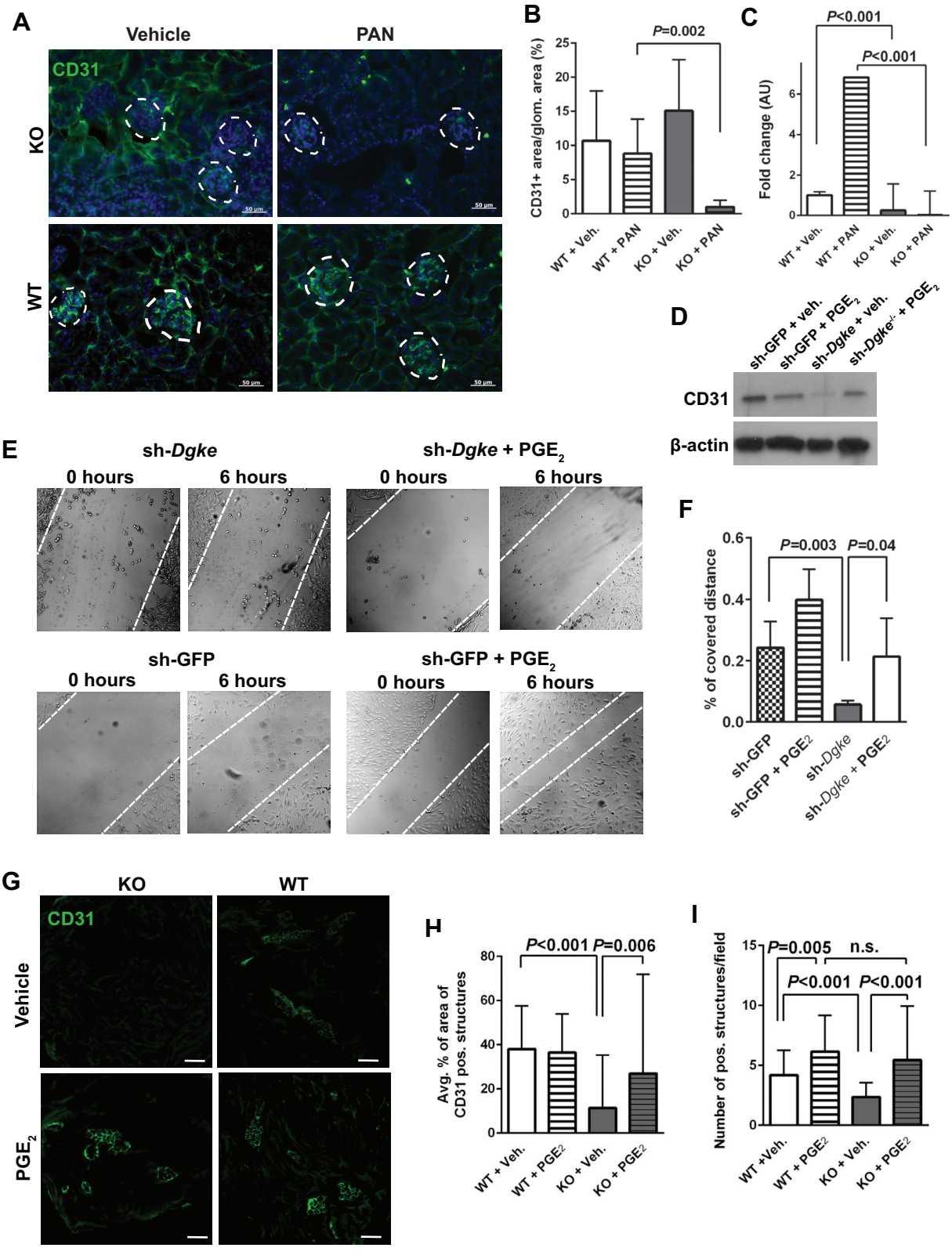

lium and participates in the regulation of the expression of Cox-2 and the production of PGE_2 in normal glomeruli.

ACKNOWLEDGMENTS

We thank Patricia Cobo-Stark and Jessica Lucas for technical support, and Rafael Rodriguez from Medtronic Xomed for kindly providing the CF50 polyvinyl sponges.

GRANTS

M. Attanasio was supported by the National Institutes of Health (NIH) (1R01DK090326-01A1, P30DK079328-04), the Satellite Healthcare, Norman S. Coplon Extramural Research Grant, and the ASN Norman Siegel Research Award. F. Ozaltin is supported by the European Community's Seventh Framework Programme (FP7/2007-2013) (EURenOmics; Grant 2012-305608). The Nephrogenetics Laboratory at Hacettepe University was established by the Hacettepe University Infrastructure Project (Grant 06A101008). K. Topham was supported by NIH grant CA095463.

DISCLOSURES

No conflicts of interest, financial or otherwise, are declared by the author(s).

AUTHOR CONTRIBUTIONS

Author contributions: J.Z., M.C., D.L., C.R., S.-S.W., A.A.R., B.L., S.Z., B.J., Y.D., K.V., H.W., S.E., R.J.Q., M.K.T., C.M., F.O., D.K.M., N.G.B., and M.A. performed experiments; J.Z., M.C., D.L., S.-S.W., A.A.R., B.L., X.J.Z., N.G.B., and M.A. analyzed data; J.Z., M.C., D.L., and M.A. interpreted results of experiments; J.Z., M.C., D.L., and M.A. edited and revised manuscript; J.Z., M.C., D.L., A.A.R., B.L., and M.A. approved final version of manuscript; D.L. and M.A. drafted manuscript; M.A. conception and design of research; M.A. prepared figures.

REFERENCES

1. **Bruneau S, Neel M, Roumenina LT, Frimat M, Laurent L, Fremeaux-Bacchi V, Fakhouri F.** Loss of DGKepsilon induces endothelial cell activation and death independently of complement activation. *Blood* 125: 1038–1046, 2015.
2. **Chen A, Wei CH, Sheu LF, Ding SL, Lee WH.** Induction of proteinuria by adriamycin or bovine serum albumin in the mouse. *Nephron* 69: 293–300, 1995.
3. **Cheng H, Fan X, Guan Y, Moeckel GW, Zent R, Harris RC.** Distinct roles for basal and induced COX-2 in podocyte injury. *J Am Soc Nephrol* 20: 1953–1962, 2009.
4. **Cheng H, Wang S, Jo YI, Hao CM, Zhang M, Fan X, Kennedy C, Breyer MD, Moeckel GW, Harris RC.** Overexpression of cyclooxygenase-2 predisposes to podocyte injury. *J Am Soc Nephrol* 18: 551–559, 2007.
5. **Cruz-Gervis R, Stecenko AA, Dworski R, Lane KB, Loyd JE, Pierson R, King G, Brigham KL.** Altered prostanoid production by fibroblasts cultured from the lungs of human subjects with idiopathic pulmonary fibrosis. *Respir Res* 3: 17, 2002.
6. **DeLisser HM, Christofidou-Solomidou M, Strieter RM, Burdick MD, Robinson CS, Wexler RS, Kerr JS, Garlanda C, Merwin JR, Madri JA, Albelda SM.** Involvement of endothelial PECAM-1/CD31 in angiogenesis. *Am J Pathol* 151: 671–677, 1997.
7. **Edwards RM.** Effects of prostaglandins on vasoconstrictor action in isolated renal arterioles. *Am J Physiol Renal Fluid Electrolyte Physiol* 248: F779–F784, 1985.
8. **Falati S, Patil S, Gross PL, Stapleton M, Merrill-Skoloff G, Barrett NE, Pixton KL, Weiler H, Cooley B, Newman DK, Newman PJ, Furie BC, Furie B, Gibbins JM.** Platelet PECAM-1 inhibits thrombus formation in vivo. *Blood* 107: 535–541, 2006.
9. **Fremeaux-Bacchi V, Miller EC, Liszewski MK, Strain L, Blouin J, Brown AL, Moghal N, Kaplan BS, Weiss RA, Lhotta K, Kapur G, Mattoo T, Nivet H, Wong W, Gie S, Hurault de Ligny B, Fischbach M, Gupta R, Hauhart R, Meunier V, Loirat C, Dragon-Durey MA, Fridman WH, Janssen BJ, Goodship TH, Atkinson JP.** Mutations in complement C3 predispose to development of atypical hemolytic uremic syndrome. *Blood* 112: 4948–4952, 2008.
10. **Fu Y, Du Y, Mohan C.** Experimental anti-GBM disease as a tool for studying spontaneous lupus nephritis. *Clin Immunol* 124: 109–118, 2007.
11. **George JN, Nester CM.** Syndromes of thrombotic microangiopathy. *N Engl J Med* 371: 654–666, 2014.
12. **Hao CM, Breyer MD.** Physiological regulation of prostaglandins in the kidney. *Annu Rev Physiol* 70: 357–377, 2008.
13. **Harris RC, Breyer MD.** Physiological regulation of cyclooxygenase-2 in the kidney. *Am J Physiol Renal Physiol* 281: F1–F11, 2001.
14. **Harris RC, Mckanna JA, Homma T, Jacobson HR, Dubois RN, Breyer MD.** Cycloxygenase-2 is localized to the macula densa and papillary interstitial-cells and increases with salt restriction. *J Am Soc Nephrol* 5: 680–680, 1994.
15. **Hosler GA, Cusumano AM, Hutchins GM.** Thrombotic thrombocytopenic purpura and hemolytic uremic syndrome are distinct pathologic entities. A review of 56 autopsy cases. *Arch Pathol Lab Med* 127: 834–839, 2003.
16. **Jo YI, Cheng H, Wang S, Moeckel GW, Harris RC.** Puromycin induces reversible proteinuric injury in transgenic mice expressing cyclooxygenase-2 in podocytes. *Nephron Exp Nephrol* 107: e87–e94, 2007.
17. **Keir L, Coward RJ.** Advances in our understanding of the pathogenesis of glomerular thrombotic microangiopathy. *Pediatr Nephrol* 26: 523–533, 2011.
18. **Komhoff M, Grone HJ, Klein T, Seyberth HW, Nusing RM.** Localization of cyclooxygenase-1 and -2 in adult and fetal human kidney: implication for renal function. *Am J Physiol Renal Physiol* 272: F460–F468, 1997.
19. **Kunze H, Vogt W.** Significance of phospholipase A for prostaglandin formation. *Ann N Y Acad Sci* 180: 123–125, 1971.
20. **Lemaire M, Fremeaux-Bacchi V, Schaefer F, Choi MR, Tang WH, Le Quintrec M, Fakhouri F, Taque S, Nobili F, Martinez F, Ji WZ, Overton JD, Mane SM, Nurnberg G, Altmuller J, Thiele H, Morin D, Deschenes G, Baudouin V, Llanas B, Collard L, Majid MA, Simkova E, Nurnberg P, Rioux-Leclerc N, Moeckel GW, Gubler MC, Hwa J, Loirat C, Lifton RP.** Recessive mutations in DGKE cause atypical hemolytic-uremic syndrome. *Nat Genet* 45: 531–536, 2013.
21. **Li B, Rauhauser AA, Dai J, Sakthivel R, Igarashi P, Jetten AM, Attanasio M.** Increased hedgehog signaling in postnatal kidney results in aberrant activation of nephron developmental programs. *Hum Mol Genet* 20: 4155–4166, 2011.
22. **Lukiw WJ, Cui JG, Musto AE, Musto BC, Bazan NG.** Epileptogenesis in diacylglycerol kinase epsilon deficiency up-regulates COX-2 and tyrosine hydroxylase in hippocampus. *Biochem Biophys Res Commun* 338: 77–81, 2005.
23. **Masoodi M, Nicolaou A.** Lipidomic analysis of twenty-seven prostanoids and isoprostanes by liquid chromatography/electrospray tandem mass spectrometry. *Rapid Commun Mass Spectrom* 20: 3023–3029, 2006.
24. **Merida I, Avila-Flores A, Merino E.** Diacylglycerol kinases: at the hub of cell signalling. *Biochem J* 409: 1–18, 2008.
25. **Milne SB, Ivanova PT, Armstrong MD, Myers DS, Lubarda J, Shulga YV, Topham MK, Brown HA, Epand RM.** Dramatic differences in the roles in lipid metabolism of two isoforms of diacylglycerol kinase. *Biochemistry* 47: 9372–9379, 2008.
26. **Morigi M, Galbusera M, Gastoldi S, Locatelli M, Buelli S, Pezzotta A, Pagani C, Noris M, Gobbi M, Stravalaci M, Rottoli D, Tedesco F, Remuzzi G, Zoja C.** Alternative pathway activation of complement by Shiga toxin promotes exuberant C3a formation that triggers microvascular thrombosis. *J Immunol* 187: 172–180, 2011.
27. **Murakami M, Naraba H, Tanioka T, Semmyo N, Nakatani Y, Kojima F, Ikeda T, Fueki M, Ueno A, Oh S, Kudo I.** Regulation of prostaglandin E2 biosynthesis by inducible membrane-associated prostaglandin E2 synthase that acts in concert with cyclooxygenase-2. *J Biol Chem* 275: 32783–32792, 2000.
28. **Namkoong S, Lee SJ, Kim CK, Kim YM, Chung HT, Lee H, Han JA, Ha KS, Kwon YG, Kim YM.** Prostaglandin E2 stimulates angiogenesis by activating the nitric oxide/cGMP pathway in human umbilical vein endothelial cells. *Exp Mol Med* 37: 588–600, 2005.
29. **Noris M, Mele C, Remuzzi G.** Podocyte dysfunction in atypical haemolytic uraemic syndrome. *Nat Rev Nephrol* 11: 245–252, 2015.
30. **Noris M, Remuzzi G.** Atypical hemolytic-uremic syndrome. *N Engl J Med* 361: 1676–1687, 2009.
31. **Ozaltin F, Li BH, Rauhauser A, An SW, Soylemezoglu O, Gonul II, Taskiran EZ, Ibsirlioglu T, Korkmaz E, Bilginer Y, Duzova A, Ozen S, Topaloglu R, Besbas N, Ashraf S, Du Y, Liang CY, Chen P, Lu DM, Vadnagara K, Arbuckle S, Lewis D, Wakeland B, Quigg RJ, Ransom RF, Wakeland EK, Topham MK, Bazan NG, Mohan C, Hildebrandt F, Bakkaloglu A, Huang CL, Attanasio M.** DGKE variants cause a glomerular microangiopathy that mimics membranoproliferative GN. *J Am Soc Nephrol* 24: 377–384, 2013.

32. **Pozzi A, Macias-Perez I, Abair T, Wei S, Su Y, Zent R, Falck JR, Capdevila JH.** Characterization of 5,6- and 8,9-epoxyeicosatrienoic acids (5,6- and 8,9-EET) as potent in vivo angiogenic lipids. *J Biol Chem* 280: 27138–27146, 2005.
33. **Qi Z, Cai H, Morrow JD, Breyer MD.** Differentiation of cyclooxygenase 1- and 2-derived prostanoids in mouse kidney and aorta. *Hypertension* 48: 323–328, 2006.
34. **Rao R, Redha R, Macias-Perez I, Su Y, Hao C, Zent R, Breyer MD, Pozzi A.** Prostaglandin E2-EP4 receptor promotes endothelial cell migration via ERK activation and angiogenesis in vivo. *J Biol Chem* 282: 16959–16968, 2007.
35. **Riedl M, Fakhouri F, Le Quintrec M, Noone DG, Jungraithmayr TC, Fremeaux-Bacchi V, Licht C.** Spectrum of complement-mediated thrombotic microangiopathies: pathogenetic insights identifying novel treatment approaches. *Semin Thromb Hemost* 40: 444–464, 2014.
36. **Rodriguez de Turco EB, Tang W, Topham MK, Sakane F, Marcheselli VL, Chen C, Taketomi A, Prescott SM, Bazan NG.** Diacylglycerol kinase epsilon regulates seizure susceptibility and long-term potentiation through arachidonoyl- inositol lipid signaling. *Proc Natl Acad Sci U S A* 98: 4740–4745, 2001.
37. **Schlondorff D, Ardaillou R.** Prostaglandins and other arachidonic acid metabolites in the kidney. *Kidney Int* 29: 108–119, 1986.
38. **Smith WL, Langenbach R.** Why there are two cyclooxygenase isozymes. *J Clin Invest* 107: 1491–1495, 2001.
39. **Steffel J, Luscher TF, Ruschitzka F, Tanner FC.** Cyclooxygenase-2 inhibition and coagulation. *J Cardiovasc Pharmacol* 47, *Suppl* 1: S15–S20, 2006.
40. **Stitt-Cavanagh EM, Faour WH, Takami K, Carter A, Vanderhyden B, Guan Y, Schneider A, Breyer MD, Kennedy CR.** A maladaptive role for EP4 receptors in podocytes. *J Am Soc Nephrol* 21: 1678–1690, 2010.
41. **Tang W, Bunting M, Zimmerman GA, McIntyre TM, Prescott SM.** Molecular cloning of a novel human diacylglycerol kinase highly selective for arachidonate-containing substrates. *J Biol Chem* 271: 10237–10241, 1996.
42. **Westland R, Bodria M, Carrea A, Lata S, Scolari F, Fremeaux-Bacchi V, D'Agati VD, Lifton RP, Gharavi AG, Ghiggeri GM, Sanna-Cherchi S.** *Phenotypic* Expansion of DGKE-Associated Diseases. *J Am Soc Nephrol* 25: 1408–1414, 2014.
43. **Xie C, Sharma R, Wang H, Zhou XJ, Mohan C.** Strain distribution pattern of susceptibility to immune-mediated nephritis. *J Immunol* 172: 5047–5055, 2004.
44. **Zinellu A, Caria MA, Tavera C, Sotgia S, Chessa R, Deiana L, Carru C.** Plasma creatinine and creatine quantification by capillary electrophoresis diode array detector. *Anal Biochem* 342: 186–193, 2005.